analytical chemistry

pubs.acs.org/ac Letter

Simultaneous Quantification of H_2O_2 and Organic Hydroperoxides by ^1H NMR Spectroscopy

Tayeb Kakeshpour and Ad Bax*

Cite This: *Anal. Chem.* 2022, 94, 5729−5733 Read Online

ACCESS | Metrics & More | Article Recommendations | Supporting Information

ABSTRACT: Due to similar reactivity of organic hydroperoxides (OHPs), an HPLC separation step is typically required for their indirect (chemical) quantification in mixtures. The high sensitivity of chemical shifts to chemical structure makes NMR an ideal tool for the simultaneous quantification of OHPs in mixtures, but the concentration of these analytes in the samples of interest is usually well below the sensitivity of standard NMR experiments. This sensitivity problem can be mitigated by taking advantage of the fact that the z magnetization of the H_2O_2 resonance recovers at the rate of hydrogen exchange with water, which is significantly faster than longitudinal relaxation, thus enabling very fast scanning for signal-to-noise enhancement. An adaptation of the *E-BURP2* pulse is described that suppresses the water signal by more than 4 orders of magnitude, yielding uniform excitation of peroxide signals without interference of the ca. 10^8-fold stronger H_2O resonance. We demonstrate the method for a mixture of OHPs and report the chemical shifts for multiple OHPs that are of interest in atmospheric chemistry. As shown for hydroxymethyl hydroperoxide, the chemical decay of OHPs can be tracked directly by NMR spectroscopy.

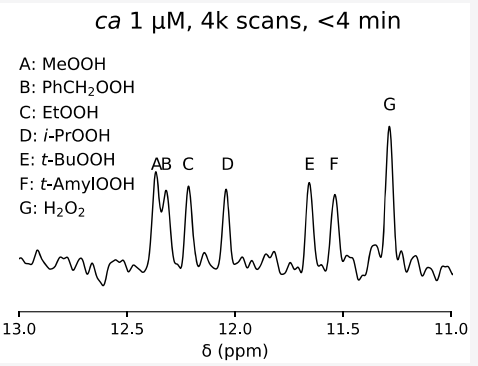

This Letter extends the application of a recently developed NMR method for nanomolar detection of hydrogen peroxide (H_2O_2)[1,2] to organic hydroperoxides (OHPs). This class of peroxides plays key roles in many fields, ranging from synthetic[3] and atmospheric chemistry[4] to human diseases,[5] and their quantification is important from safety and product quality points of view.[6] In the atmosphere, OHPs can result from radical reactions initiated by hydrogen abstraction from saturated hydrocarbons[7] or via ozonolysis of alkenes like α-pinene,[8,9] followed by hydration of Criegee intermediates.[10] Iodometric and other chemical methods typically used for the quantification of OHPs do not distinguish them from each other or from H_2O_2 and, thus, only report the total peroxide concentration.[11] Good selectivity of the catalase enzyme for H_2O_2 vs OHPs has been utilized for the determination of total OHP concentrations in samples containing H_2O_2.[12] Post-HPLC derivatization has been used for quantification of individual OHPs down to 20 nM.[13] Although these methods can distinguish between stable hydroperoxides, they are not suitable for hydroxyalkyl hydroperoxides that decompose to their corresponding carbonyl compounds within minutes.[4] Mass spectroscopy is another sensitive method for the detection of OHPs without the need for HPLC purification;[14] however, it is inherently not a quantitative method.[15]

The facts that NMR spectroscopy is quantitative and that chemical shifts are quite sensitive to chemical structure make it a suitable method for the quantification of OHPs in mixtures. While NMR detection of the downfield shifted H_2O_2 signal (at ca. 11.3 ppm) was first reported nearly two decades ago,[16] the limited sensitivity of NMR prevented applications to OHPs in the concentration ranges that are of most practical interest. The low sensitivity of NMR, in part, originates from long interscan delays required for z magnetization recovery via longitudinal relaxation. However, for protons that exchange with water, as applies to OHPs, recovery following selective excitation of the hydroperoxide region of the spectrum (ca. 11−12.5 ppm) is dominated by hydrogen exchange (HX) with water, obviating the need for long interscan delays. Together with advances in spectrometer hardware, this now permits detection down to the nanomolar range.

EXPERIMENTAL SECTION

Validation of Commercial H_2O_2 and *t*-BuOOH Sources. ^1H NMR spectra of concentrated samples were fitted to Lorentzian functions for accurate quantification. To reduce radiation damping and receiver overload due to strong resonances in concentrated samples, the probe was detuned, the receiver gain was set to its minimum value, and a single short 1 μs pulse, corresponding to a ca. 4° flip angle, was applied followed by a 1 s acquisition. Signal integration of the

Received: January 17, 2022
Accepted: March 31, 2022
Published: April 8, 2022

https://doi.org/10.1021/acs.analchem.2c00264
Anal. Chem. 2022, 94, 5729−5733

water and solute signals confirmed all concentrations agreed to within ±1% of the manufacturer's specification (see Figure S1). We note that quantification relative to the water signal is only needed to evaluate the concentrated commercial samples (e.g., 30% H_2O_2 and 70% *t*-BuOOH). Quantification of dilute peroxide samples is easily accomplished by the standard addition of a small known quantity of such a commercial reference sample.

Organic Peroxide Synthesis. Details regarding the preparation of hydroxymethyl hydroperoxide (HMHP), benzyl hydroperoxide ($PhCH_2OOH$), isopropyl hydroperoxide (*i*-PrOOH), methyl hydroperoxide (MeOOH), ethyl hydroperoxide (EtOOH), and *tert*-amyl hydroperoxide (*t*-AmylOOH) are included in the Supporting Information. *tert*-Butyl hydroperoxide (*t*-BuOOH) was purchased from Sigma-Aldrich.

NMR. All NMR spectra were collected on a 600 MHz Bruker NEO spectrometer equipped with a cryogenic probe. Measurements were analogous to those in our earlier report,[1] but in order to prevent large frequency-dependent phase errors that interfered with baseline correction, the excitation pulse was replaced by a 2.5 ms *E-BURP2* pulse[17] that covers a bandwidth of ca. 2 ppm at 600 MHz and an offset parameter that centers its excitation at 11.8 ppm. This pulse results in a weak, spurious excitation of the on-resonance water signal, corresponding to a 1.4° flip angle. With solely this *E-BURP2* excitation, the resulting water signal remained about a million-fold stronger than a fully excited 1 μM peroxide resonance, interfering with the detection of this weak signal. This spurious water signal was reduced more than 100-fold by application of a rectangular 5 μs pulse whose RF-field strength and phase were empirically fine-tuned to negate water excitation by the *E-BURP2* pulse. The initial parameters for this rectangular pulse were first adjusted in a separate measurement that used only this pulse to yield the same amplitude and phase of the water signal as the *E-BURP2* excitation. Then, after inverting its phase, it was appended immediately after the *E-BURP2* pulse (Supporting Information). Following additional fine-tuning of the power and phase of this water flip-back pulse, an additional ca. 100-fold suppression of the water signal was obtained relative to that of just the *E-BURP2* pulse. Even after this optimization, the suppressed H_2O signal can remain several orders of magnitude more intense than low-concentration peroxide signals. To avoid truncation wiggles from the water signal in the Fourier transformed spectrum, the time domain data must be apodized to smoothly decrease to zero at the end of the free induction decay (FID). The commonly used π/2-shifted sine bell function, or its squared variant, is well suited for this purpose. Because such an apodization window does not scale the first data point of the time domain, application of the window does not alter the integrated signal intensity.

Simulated excitation profiles show that the added, small flip angle pulse applied to suppress the water peak has minimal impact on the uniformity of excitation of the hydroperoxide region. The uniformity of excitation across the hydroperoxide region was confirmed experimentally by measuring the peroxide resonance intensity of a 10 mM *t*-BuOOH sample while varying the offset frequency (Figure S2).

Chemical Shift Calculations. For each compound, a systematic conformer search was performed at the ωB97X-D/6-31G* level of theory using Spartan'20.[18] The free energies for each conformer were then calculated using the G4(MP2) composite method[19] from which the Boltzmann distribution of conformer populations was calculated using

$$p_i = \frac{e^{-G_i/RT}}{\sum_i e^{-G_i/RT}} \quad (1)$$

in which p_i and G_i are the population and calculated relative free energy of the *i*th conformer, respectively; R is the universal gas constant; T is the absolute temperature. Next, the optimized geometries obtained from the G4(MP2) calculations were checked for duplicate geometries and imaginary frequencies before being used to calculate the NMR isotropic shielding values (σ_i) using the Gauge-Independent Atomic Orbital (GIAO) method. The chemical shielding calculations were performed at the ωB97X-D[20]/aug-cc-pVDZ[21] level of theory. Boltzmann-weighted shielding values (σ_{BW}) were then derived using

$$\sigma_{BW} = \sum_i p_i \times \sigma_i \quad (2)$$

in which i runs over all conformers. Finally, the σ_{BW} values were converted to chemical shifts (δ_{calc}) using

$$\delta_{calc} = \sigma_{BW}(DSS) - \sigma_{BW} \quad (3)$$

where $\sigma_{BW}(DSS)$ is the Boltzmann-weighted isotropic shielding value for the 2,2-dimethylsilapentane-5-sulfonate (DSS) anion calculated at the same level of theory. Gaussian 16[22] was utilized for all the calculations after the conformational search, and water was simulated by SMD[23] for both thermochemical and NMR calculations. For details, see the Supporting Information.

RESULTS AND DISCUSSION

Since OHPs have pK_a values very close to that of H_2O_2,[24] they are expected to have resonances that are similar in HX rate, R_{ex}, and chemical shift. Indeed, a 1 mM sample of commercially available *t*-BuOOH shows a ^{1}H NMR resonance at 11.66 ppm, close to but readily distinguishable from that of H_2O_2. R_{ex} can be derived from transverse or longitudinal relaxation measurements,[1] but due to the absence of $^2J_{HH}$ or $^3J_{HH}$ couplings, R_{ex} is also directly reflected in the resonance line width, which for a sufficiently long acquisition time, equals R_{ex}/π Hz in the absence of apodization. At 2 °C and 1 mM MES buffer, the R_{ex} minimum of *t*-BuOOH is at pH 6.3 (Figure 1) and is the lowest (27 s^{-1}) of the OHPs investigated here, only moderately slower than that of H_2O_2 (41 s^{-1}).[1] With the R_{ex} rates and their pH dependence being comparable for OHPs and H_2O_2, their NMR intensities therefore can be quantified simultaneously on a single sample.

With multiple peroxide resonances in a single spectrum, the strong linearly offset-dependent phase correction associated with the originally used Gaussian-shaped pulse[1] resulted in severe baseline undulations, and an *E-BURP2* pulse followed by a very weak water flip-back pulse was used instead (see Experimental Section). The excitation profile of this pulse pair is flat to within ±2% over a 2 ppm bandwidth (Figure S2), thus providing full excitation of all OHP resonances.

All observed OHP signals resonate downfield of H_2O_2 and have unique chemical shifts (Figure 2). Their chemical shifts relative to 2,2-dimethylsilapentane-5-sulfonic acid (DSS) are listed in Table 1. The comparison of H_2O_2 and MeOOH shows that the addition of one methyl group results in a substantial chemical shift change (11.29 vs 12.37 ppm). This

https://doi.org/10.1021/acs.analchem.2c00264
Anal. Chem. 2022, 94, 5729−5733

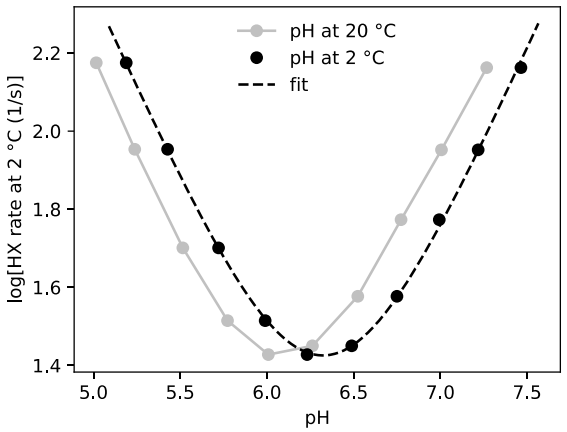

Figure 1. pH dependence of the *t*-BuOOH HX rate with water in samples containing 1 mM MES and 1 mM *t*-BuOOH. The pH of the samples was adjusted at 20 °C, and the rates were measured at 2 °C. The pH values at 2 °C were calculated via two-point extrapolation from pH measurements at 20 and 5 °C. The dashed line represents the best fit to $k_{ex} = k_{H2O} + k_{MES}[MES] + k_H10^{-pH} + k_{OH}10^{-pOH}$, in which k_{H2O}, k_{MES}, k_H, and k_{OH} are water-, MES-, acid-, and base-catalyzed rate constants, respectively, and their best-fitted values are $k_{H2O} + k_{MES}[MES] = 5.7 \pm 0.6$ $M^{-1}s^{-1}$; $k_H = (2.2 \pm 0.1) \times 10^7$ $M^{-1}s^{-1}$; $k_{OH} = (3.6 \pm 0.1) \times 10^9$ $M^{-1}s^{-1}$.

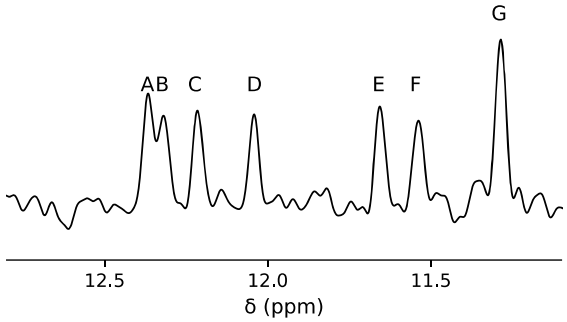

Figure 2. Downfield region of the 600 MHz ^{1}H NMR spectrum for a mixture of H_2O_2 and six OHPs, all at ca. 1 μM concentration in 1 mM MES. The pH of the sample was adjusted to 6.0 at 20 °C using a glass electrode, and the spectra were collected at 2 °C. The spectrum was collected using 4096 scans (4 min), an acquisition time of 50 ms, and an interscan delay of 1 ms. The FID was apodized by a $\pi/2$-shifted sine bell function. Resonances correspond to (A) MeOOH; (B) $PhCH_2OOH$; (C) EtOOH; (D) *i*-PrOOH; (E) *t*-BuOOH; (F) *t*-AmylOOH; (G) H_2O_2. For spectra of the individual OHPs, see Figure S3.

Table 1. Calculated vs Experimental ^{1}H Chemical Shifts

compound	exp δ (ppm)[a]	calc'd δ (ppm)[a,b]
H_2O_2	11.29	7.68
HMHP	12.42	8.60
MeOOH	12.37	8.29
$PhCH_2OOH$	12.31	8.18
EtOOH	12.22	8.12
i-PrOOH	12.04	7.84
t-BuOOH	11.66	7.43
t-AmylOOH	11.54	7.32

[a]Referenced vs DSS. [b]Boltzmann-weighted values using G4(MP2)/SMD free energies and ωB97X-D/aug-cc-pVDZ/SMD NMR calculations.

chemical shift difference is in the same direction but larger than what is obtained from DFT simulations (Table 1, also referenced to DSS). After the methyl addition, the addition of alkyl groups to the α carbon results in smaller upfield chemical shift changes, making primary, secondary, and tertiary OHPs readily distinguishable from one another. The comparison of *t*-BuOOH and *t*-AmylOOH chemical shifts shows that even relatively remote substitution on beta carbons can result in distinguishable chemical shifts. Although the calculated absolute values for chemical shifts are off by a few ppm, there generally is a fair correlation between calculated and experimental chemical shifts with only one outlier, H_2O_2 (Figure 3). This disagreement may result from the difference in solvation of the small and polar H_2O_2 molecule vs OHPs.

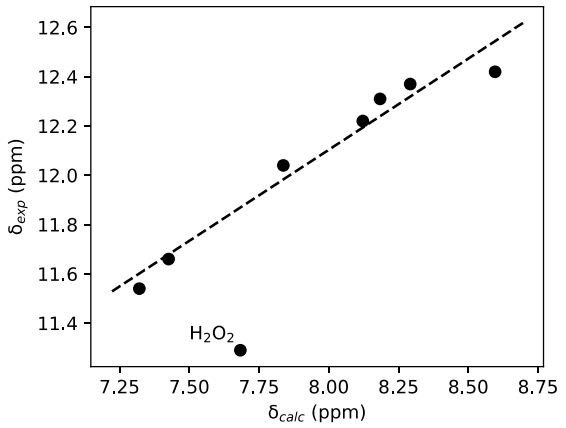

Figure 3. Correlation between experimental and calculated chemical shifts. The slope and intercept are 0.74 ± 0.07 and 6.2 ± 0.6 ppm, respectively.

Hydroxyalkyl hydroperoxides such as HMHP are of interest in atmospheric chemistry. HMHP is thought to be mostly produced in the atmosphere through ozonolysis of terminal alkenes, followed by hydration of a Criegee intermediate.[25] Once in the condensed phase, however, these compounds will decompose to their corresponding carbonyl compounds and H_2O_2. This reaction can be readily tracked by NMR (Figure 4), showing a decomposition rate of HMHP at pH 6 and 25 °C that is about 10-fold slower than prior values measured at pH 7.07 and 22 °C.[26] The decay rate is further decreased by more than 20-fold (Figure 3) when the temperature is lowered to 2 °C, indicative of a high activation energy of ca. 26 kcal/mol for this reaction at pH 6, ignoring the small sample pH change upon cooling.

CONCLUSIONS

Although NMR spectroscopy typically is not considered to be a sensitive method, when one takes advantage of the fast HX of OHPs with water, the quantification of their presence down to submicromolar concentrations within minutes is straightforward. The advantage of NMR over other methods is that chemical shifts are quite sensitive to covalent structure, resulting in unique shifts that simultaneously enable the identification of OHPs and their approximate quantification in aqueous mixtures, eliminating the need for separation associated with other detection methods. However, if precise quantitation is of the essence, we recommend that the acquisition time is increased to 100 ms, such that HX with water is essentially complete (Figure S4). If an OHP were to

https://doi.org/10.1021/acs.analchem.2c00264
Anal. Chem. 2022, 94, 5729−5733

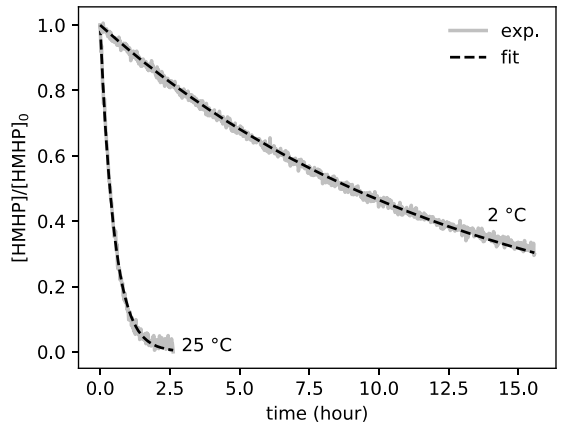

Figure 4. Degradation of HMHP at 25 and 2 °C, pH 6.0. A 10 μL portion of the reaction mixture described in the Supporting Information Synthesis Section, containing ca. 1.75 mM HMHP, was added to 490 μL of 1 mM MES buffer with 2% D_2O, pH 6.0. Spectra were collected within 5 min of mixing. Dashed lines are the best fits to the exponential decays, resulting in first order rate constants of $(5.6 \pm 0.1) \times 10^{-4}$ and $(2.1 \pm 0.1) \times 10^{-5}$ s^{-1} at 20 and 2 °C, respectively.

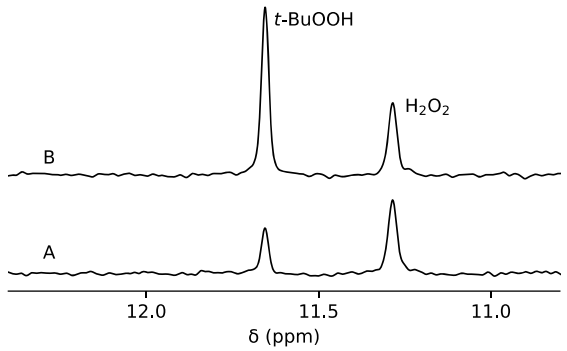

Figure 5. ^{1}H NMR spectra of a sample (A) containing 1 μM H_2O_2 and 1 μM *t*-BuOOH and (B) after the addition of 3 μM *t*-BuOOH. The ratio of the H_2O_2/*t*-BuOOH peak integrals changed from 1.00:0.50 to 1.00:2.01 upon the 3 μM addition. The uncertainty in integrations was ±30 nM (root-mean-square of baseline integrals of 12, 0.1 ppm sections in spectrum A). Samples were prepared by the serial dilution of commercial sources and verified gravimetrically with results agreeing to within 1%. The pH of the sample was adjusted to 6.0 at 20 °C, and the spectra were collected at 2 °C. The number of scans, acquisition time, and interscan delays were 16k, 100 ms, and 1 ms, respectively. The FID was apodized by a π/2-shifted sine bell squared function. A third-order polynomial baseline correction was applied manually.

have a much slower HX rate than H_2O_2, then this would be immediately apparent by its narrower line width and the measurement may need to be repeated with an even longer interscan delay. However, this did not apply for any of the OHPs in our study. We also note that the method requires H_2O as the solvent because it relies on fast HX.[1] Rapid HX was observed for all OHPs evaluated in our work, and both the adjustment of the pH to ca. 6 and lowering the temperature to just above the freezing point of water were needed to slow down the HX rates to values that yielded high resolution ^{1}H NMR spectra.

The above procedure therefore permits quantitative OHP analysis by comparison with the intensity of a known H_2O_2 reference intensity (Figure 5). We also find that the NMR peak intensity correlates well with the *t*-BuOOH concentration over a concentration range that spans 6 orders of magnitude (Figure S5).

The simple NMR pulse sequence introduced here to suppress the water signal, without requiring pulsed field gradients or echo delays, reduces excitation of the water signal by more than 4 orders of magnitude while retaining full intensity for the resonances selected by the band-selective excitation pulse. The good correlation between experimental peroxide ^{1}H chemical shifts and quantum−mechanical calculations will aid in the identification of unknown compounds.

■ ASSOCIATED CONTENT

Supporting Information

The Supporting Information is available free of charge at https://pubs.acs.org/doi/10.1021/acs.analchem.2c00264.

Experimental details of the OHP syntheses; NMR spectra of individual OHPs and the excitation profile of the *E-BURP2*/flip-back pulse pair; Cartesian coordinates of the optimized structures; calculated thermodynamic parameters and isotropic shielding values; NMR pulse program (PDF)

■ AUTHOR INFORMATION

Corresponding Author

Ad Bax − *Laboratory of Chemical Physics, NIDDK, National Institutes of Health, Bethesda, Maryland 20892, United States;* orcid.org/0000-0002-9809-5700; Email: bax@nih.gov

Author

Tayeb Kakeshpour − *Laboratory of Chemical Physics, NIDDK, National Institutes of Health, Bethesda, Maryland 20892, United States*

Complete contact information is available at: https://pubs.acs.org/10.1021/acs.analchem.2c00264

Notes

The authors declare no competing financial interest.

■ ACKNOWLEDGMENTS

The authors thank James Baber and Jinfa Ying for technical support and Dennis A. Torchia for helpful discussions. The authors also thank David Hoover at the NIH Biowulf high-performance computing center for technical support. This work was supported by the Intramural Research Program of the National Institute of Diabetes and Digestive and Kidney Diseases.

■ REFERENCES

(1) Kakeshpour, T.; Bax, A. *J. Magn. Reson.* **2021**, *333*, 107092.
(2) Kakeshpour, T.; Metaferia, B.; Zare, R. N.; Bax, A. *Proc. Natl. Acad. Sci. U. S. A.* **2022**, *119* (8), No. e2121542119.
(3) Hill, J. G.; Sharpless, K. B.; Exon, C. M.; Regenye, R. *Organic Synthesis* **1985**, *63*, 66.
(4) Enami, S. *J. Phys. Chem. A* **2021**, *125* (21), 4513−4523.
(5) Miyamoto, S.; Ronsein, G. E.; Prado, F. M.; Uemi, M.; Corrêa, T. C.; Toma, I. N.; Bertolucci, A.; Oliveira, M. C. B.; Motta, F. D.; Medeiros, M. H. G.; Mascio, P. D. *IUBMB Life* **2007**, *59* (4−5), 322−331.
(6) Kelly, R. J. *Chemical Health Safety* **1996**, *3* (5), 28−36.
(7) Atkinson, R. *Chem. Rev.* **1986**, *86* (1), 69−201.

(8) Taatjes, C. A.; Meloni, G.; Selby, T. M.; Trevitt, A. J.; Osborn, D. L.; Percival, C. J.; Shallcross, D. E. *J. Am. Chem. Soc.* **2008**, *130* (36), 11883−11885.
(9) Taatjes, C. A.; Welz, O.; Eskola, A. J.; Savee, J. D.; Scheer, A. M.; Shallcross, D. E.; Rotavera, B.; Lee, E. P. F.; Dyke, J. M.; Mok, D. K. W.; Osborn, D. L.; Percival, C. J. *Science* **2013**, *340* (6129), 177−180.
(10) Chao, W.; Hsieh, J.-T.; Chang, C.-H.; Lin, J.-M. *Science* **2015**, *347* (6223), 751−754.
(11) Cheeseman, J. M. *J. Exp. Bot.* **2006**, *57* (10), 2435−2444.
(12) Gere, E. P.; Bérczi, B.; Simándi, P.; Wittmann, G.; Dombi, A. *Int. J. Environ. Anal. Chem.* **2002**, *82* (7), 443−450.
(13) Kok, G. L.; McLaren, S. E.; Staffllbach, T. A. *Journal of Atmospheric and Oceanic Technology* **1995**, *12* (2), 282−289.
(14) Zhou, S.; Rivera-Rios, J. C.; Keutsch, F. N.; Abbatt, J. P. D. *Atmos. Meas. Technol.* **2018**, *11* (5), 3081−3089.
(15) Bantscheff, M.; Schirle, M.; Sweetman, G.; Rick, J.; Kuster, B. *Anal. Bioanal. Chem.* **2007**, *389* (4), 1017−1031.
(16) Stephenson, N. A.; Bell, A. T. *Anal. Bioanal. Chem.* **2005**, *381* (6), 1289−1293.
(17) Geen, H.; Freeman, R. *J. Magn. Reson.* **1991**, *93*, 93−141.
(18) *Spartan'20*; Wavefunction Inc.: Irvine, CA, USA, 2020.
(19) Curtiss, L. A.; Redfern, P. C.; Raghavachari, K. *J. Chem. Phys.* **2007**, *127* (12), 124105.
(20) Chai, J.-D.; Head-Gordon, M. *Phys. Chem. Chem. Phys.* **2008**, *10* (44), 6615−6620.
(21) Dunning, T. H. *J. Chem. Phys.* **1989**, *90* (2), 1007−1023.
(22) Frisch, M. J.; Trucks, G. W.; Schlegel, H. B.; Scuseria, G. E.; Robb, M. A.; Cheeseman, J. R.; Scalmani, G.; Barone, V.; Petersson, G. A.; Nakatsuji, H.; Li, X.; Caricato, M.; Marenich, A. V.; Bloino, J.; Janesko, B. G.; Gomperts, R.; Mennucci, B.; Hratchian, H. P.; Ortiz, J. V.; Izmaylov, A. F.; Sonnenberg, J. L.; Williams-Young, D.; Ding, F.; Lipparini, F.; Egidi, F.; Goings, J.; Peng, B.; Petrone, A.; Henderson, T.; Ranasinghe, D.; Zakrzewski, V. G.; Gao, J.; Rega, N.; Zheng, G.; Liang, W.; Hada, M.; Ehara, M.; Toyota, K.; Fukuda, R.; Hasegawa, J.; Ishida, M.; Nakajima, T.; Honda, Y.; Kitao, O.; Nakai, H.; Vreven, T.; Throssell, K.; Montgomery, J. A., Jr.; Peralta, J. E.; Ogliaro, F.; Bearpark, M. J.; Heyd, J. J.; Brothers, E. N.; Kudin, K. N.; Staroverov, V. N.; Keith, T. A.; Kobayashi, R.; Normand, J.; Raghavachari, K.; Rendell, A. P.; Burant, J. C.; Iyengar, S. S.; Tomasi, J.; Cossi, M.; Millam, J. M.; Klene, M.; Adamo, C.; Cammi, R.; Ochterski, J. W.; Martin, R. L.; Morokuma, K.; Farkas, O.; Foresman, J. B.; Fox, D. J. *Gaussian 16*; Revision C.01; Gaussian, Inc.: Wallingford, CT, 2016.
(23) Marenich, A. V.; Cramer, C. J.; Truhlar, D. G. *J. Phys. Chem. B* **2009**, *113* (18), 6378−6396.
(24) Kato, S. i.; Ishihara, T.; Mashio, F. *Bull. Japan Petr. Inst.* **1970**, *12*, 117−122.
(25) Neeb, P.; Sauer, F.; Horie, O.; Moortgat, G. K. *Atmos. Environ.* **1997**, *31* (10), 1417−1423.
(26) Zhou, X.; Lee, Y. N. *J. Phys. Chem.* **1992**, *96* (1), 265−272.

https://doi.org/10.1021/acs.analchem.2c00264
Anal. Chem. 2022, 94, 5729−5733